

Synthesis of morphology-controlled silver nanostructures by electrodeposition

C. L. Liang¹, K. Zhong², M. Liu², L. Jiang², S. K. Liu², D. D. Xing², H. Y. Li², Y. Na², W. X. Zhao¹, Y.

X. Tong^{2,*} and P. Liu^{2,*}

Nanostructured silver was obtained by potentiostatic electrolysis. The effects of ionized surfactant (sodium dodecanesulphonate) and the substrate (Cu and Ti) on the morphology of depositions were investigated. It is found that morphologies of silver nanostructures can be simply controlled via change of the substrate. Spherical Ag nanoparticles with narrow size distribution were obtained by electrodeposition in AgNO₃-SDS aqueous solution on copper substrate. In the case of titanium substrate, silver dendrite structures were obtained. Despite of different morphologies, XRD and TEM results showed that the as-prepared samples belong to face-centered cubic silver structure with good crystallinity. The formation mechanism of different silver nanostructures was discussed.

Keywords: Electrodeposition; Silver nanopartilces; Silver nano dendrites

Citation: C. Liang, K. Zhong, M. Liu, L. Jiang, S. Liu, D. Xing, H. Li, Y. Na, W. Zhao, Y. Tong and P. Liu, "Synthesis of morphology-controlled silver nanostructures by electrodeposition", Nano-Micro Lett. 2, 6-10 (2010). doi: [10.5101/nml.v2i1.p6-10](https://doi.org/10.5101/nml.v2i1.p6-10)

Nanometer-sized metal structures have recently attracted great interests because of their excellent electronic, magnetic, optical, thermal and catalytic properties [1-4]. It is well known that the properties of a noble metal nanostructure depend on its size, shape, morphology and crystallinity [5-8]. Therefore, much attention has been focused on the size and shape-controlled synthesis of metal nanostructures. Among many different metal nanostructures, silver nanocrystals seem to be particularly attractive because of their unique applications in active catalysts, nonlinear optical materials, electrical and thermal conductivities [9-11]. Silver nanoparticles with diameter under 20 nm exhibit effective antibacterial properties without side-effects and antibiotic resistance [12,13]. Nanoprism structure and nanodisks of silver exhibit optical properties different from the silver nanospheres, showing a potential application in optics [14,15]. Dendritic silver structure was developed as a novel good reproducible surface enhanced Raman scattering active substrate which can reflect different SERS effects based on different sizes of the dendrites [16-19]. Accordingly, by adjusting sizes and shapes in the process of synthesis, the physical and chemical properties of silver nanostructure can be

controlled.

Much effort has been made to design nanocrystals with well defined sizes, shapes and crystallinity. Until now, a number of different techniques, including electrochemical deposition [20,21], γ -irradiation route [22,23], template approach [24,25], thermal evaporation and chemical vapor deposition [26,27] have been used for growing silver nanostructures. Electrochemical deposition is relatively a simple and convenient way to synthesize silver nanostructures [28]. There are already several reports on the synthesis of silver nanostructures by electrochemical deposition [29-31]. The method generally involves the reduction of Ag salt in the presence of a suitable non-ionized surfactant. Zhu Junjie et al. [31] have prepared shaped silver particles in the presence of nitrilotriacetate (NTA) by pulse sonoelectrochemical method. Kang Zhenhui et al. [32] have reported the synthesis of Ag dendritic structure in the presence of polyethylene glycol (PEG) by electro reduction of AgNO₃. Zhu and co-workers [33] have also prepared Ag dendrites in the presence of DNA by the same technique. The effect of reaction time and concentration of both AgNO₃ and surfactant on the morphology have been discussed in literatures.

¹Instrumental Analysis & Research Center, Sun Yat-sen University

²School of Chemistry and Chemical Engineering, Sun Yat-sen University

*Corresponding author. E-mail: chedhx@mail.sysu.edu.cn, chedhx@mail.sysu.edu.cn. Telephone: +86-20-84110071

However, fewer references reported their preparation in the assisted of ionized surfactant. The effect of the substrate on the morphology of Ag nanostructures is still unknown. Moreover, the exploration of an effective and readily adoptable method for the preparation of Ag nanostructure with well-defined sized and tunable morphologies remains a challenge.

In this paper we report a surfactant assisted electrochemical deposition method to synthesize silver nanoparticles with a narrow size distribution and dendrite nanostructure. The influences of the sodium dodecylsulfonate (SDS) and the substrates (Cu and Ti) on the morphology of silver nanostructures were investigated. SEM, TEM, and XRD analysis have been used to characterize the as-prepared samples.

All chemical reagents used are analytically pure. The electrochemical cell was an H-shaped glass cell in which the anode and cathode chamber was isolated by sintered glass. The Pt film (99.9%, 0.1 cm²) and graphite rod (spectrographically pure) were used as working electrode and counter electrode, respectively. The reference electrode was a saturated calomel electrode (SCE), which has a Luggin capillary filled with asbestos fiber at the tip.

A 5×10^{-3} mol L⁻¹ AgNO₃ and a 0.2 g L⁻¹ SDS were mixed in an aqueous solution. Products were grown by potentiostatic electrolysis at room temperature. The substrates Cu and Ti were immersed into AgNO₃-SDS aqueous solution, respectively. The as-deposited samples were washed by acetone to remove surfactants and H₂O adhered to the surface.

The electrochemical measurements were performed by a Voltalab 80 universal electrochemical instrument (Radiometer Analytical) under Ar atmosphere. The surface morphology was examined by scanning electron microscope (SEM, Quanta 400F, FEI). The phase and structure of the samples were determined by X-ray diffraction (XRD, D/MAX-3A, Rigaku International Corp. Ltd.) and transmission electron microscopy (TEM, JEM-2010HR).

X-ray diffraction (XRD) measurement was carried out to determine the crystal structure of electrodeposited products. Figure 1 shows the XRD patterns of the as-deposited products. The lattice parameters determined from the diffraction peaks can be indexed to diffraction from the (111), (200), (220), (311) and (222) planes of face-centered cubic (fcc) structure of silver (JCPDS file no. 4-783).

Figure 2a shows the cyclic voltammogram (CV) of a Pt electrode in AgNO₃-SDS aqueous solution at the scan rate of

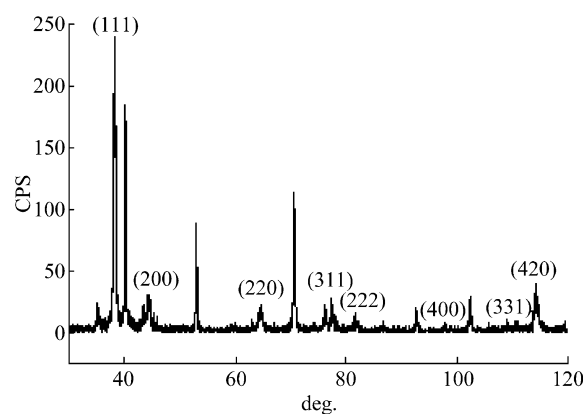


FIG. 1. XRD pattern of electrodeposited products.

100 mV s⁻¹. The voltammetric scan was commenced at 0.30 V and swept negatively. A single cathodic wave appeared at -0.22 V. On the reverse sweep, an anodic peak was observed at 0.17 V. Figure 2b shows the cyclic voltammogram (CV) of a Pt electrode in AgNO₃ aqueous solution. A single cathodic peak was at -0.13 V, and an anodic peak was 0.11 V. After the potentiostatic electrolysis was carried out, black deposits were obtained. XRD analysis confirmed that the deposits belong to face-centered cubic structure of silver. Therefore, the cathodic wave is produced due to the reduction of Ag (I) to Ag and the anodic peak accords with the anodic stripping of Ag. The reduction potential of Ag (I) shifted negatively from -0.13 V (as shown in Fig. 2b) to -0.22 V (as shown in Fig. 2a) when the SDS was presented in solution. This result indicated that nucleation process of Ag may be influenced by SDS.

Figure 3a shows the particle size and the morphologies of the deposits obtained in AgNO₃-SDS aqueous solution on a Cu plate by potentiostatic electrochemical deposition. Well dispersed spherical Ag nanoparticles with uniform granularity were observed on the substrate. The average size is measured to be 32 nm. There is a relatively narrow particle size distribution, with most of particles within 30 to 35 nm accounting for 85% of the total amount of Ag nanoparticles (as shown in Fig. 3b). The typical diameter is about 30 nm.

The detailed structural information of Ag nanoparticles was provided by TEM. Figure 4 shows a typical TEM image of Ag nanoparticles at a low magnification and the corresponding selected-area electron diffraction (SAED) pattern. In Fig. 4, the nanoparticles have dimensions in the range of 25 nm to 40 nm,

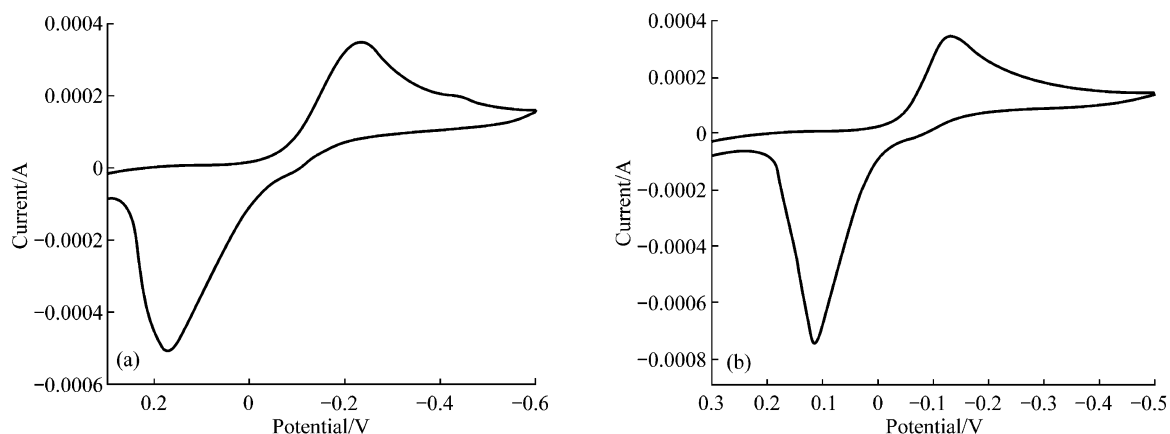


FIG. 2. CV of a Pt electrode (0.1 cm²) in AgNO₃ (5×10^{-3} mol L⁻¹) aqueous solution at the scan rate of 100 mV s⁻¹: (a) with SDS (0.2 g L⁻¹), (b) without SDS.

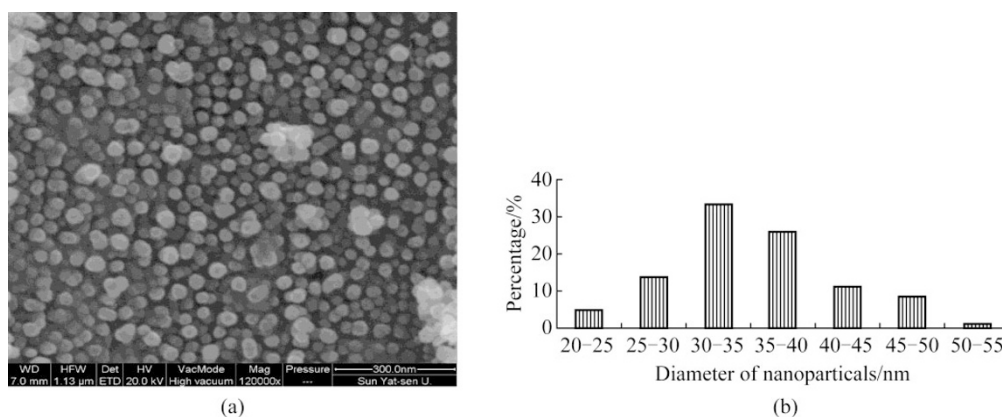


FIG. 3. (a) SEM image of the as-deposits obtained by potentiostatic electrolysis on the Cu plate at -3.00 V for 30 min in AgNO_3 (5×10^{-3} mol L^{-1})-SDS (0.2 g L^{-1}) aqueous solution (b) Histogram showing size distribution of Ag nanoparticles.

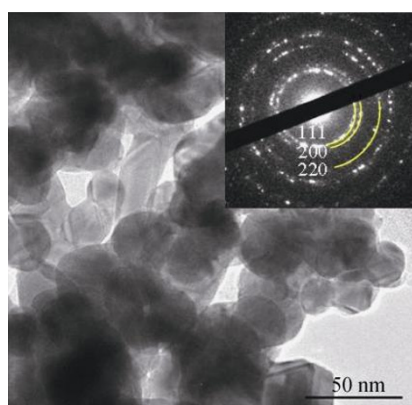


FIG. 4. TEM image of Ag nanoparticles and the corresponding SAED pattern.

which is in agreement with the results of SEM. From the study of the SAED pattern, the diffraction rings can be indexed to 111, 200 and 220 diffraction of face-centered cubic structure of silver. The shape and intensity of diffraction rings indicate that the nanoparticles are of high crystallinity.

Figure 5a shows a typical TEM image of an individual Ag nanoparticle. The corresponding SAED pattern (as shown in Fig. 5b) can be indexed as the [001] zone axis of single crystal fcc silver, and this implies that the as-prepared nanoparticles are single crystalline. HRTEM image (as shown in Fig. 5c) of the square region in Fig. 5a shows continuous single directional lattice fringes. The marked d-spacing of 0.205 nm corresponds to the interplanar distance of Ag {200} lattice planes. The HRTEM and SAED results further confirmed that the Ag nanoparticles adopt a single crystal structure with a face-centered cubic phase.

To investigate the effect of SDS on the morphology of the resulting product, a SDS-free solution growth process was carried out. The shape and size of the deposits were revealed by SEM. As shown in Fig. 6, the as-deposited products are tower-like structures. It can be seen that the basic building units of the tower structures are nanoparticles and nanoplates. It is apparent that some of them aggregate to form the tower-like structure. The bottom diameter of the particle-aggregated tower is about 110 nm, and the top diameter is about 35 nm. The corresponding XRD diffraction pattern confirmed that the nanotower structure is face-centered cubic silver. On the base of the experiments, SDS plays a key role in the formation of Ag

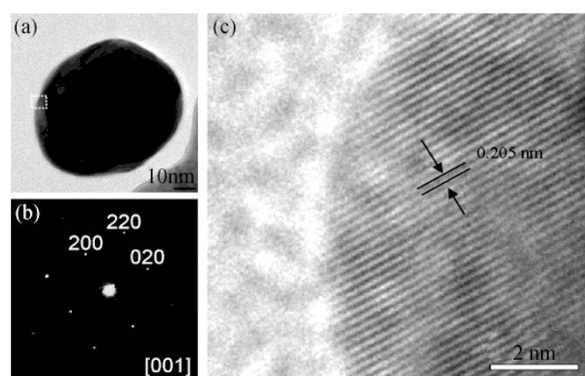


FIG. 5. (a) TEM image showing a Ag nanoparticle, (b) Indexed SAED pattern taken along [001] zone axis, and (c) HRTEM image obtained from the square region in (a).

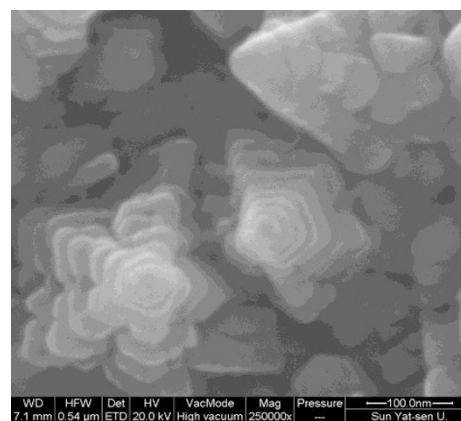


FIG. 6. SEM image of the as-deposits obtained in SDS-free solution.

nanoparticles. It is reported that [34-36] suitable surfactant may change the surface chemistry of metal particles and restrain the aggregate of metal nuclei. In our case, SDS may also be a kind of capping reagent, which absorbs on the surface of Ag particles and lowers the surface energy. Without the presence of SDS, Ag nanoparticles constructed the tower-like structure as the aggregation took place.

The growth on Ti substrate instead of Cu results in the changing from nanoparticles to dendrite structure. Figure 7a shows the representative SEM image of the as-deposited product synthesized under AgNO_3 -SDS aqueous solution by using Ti substrate. As shown in Fig. 7a, the product consists of a large amount of dendrite structures. The individual Ag

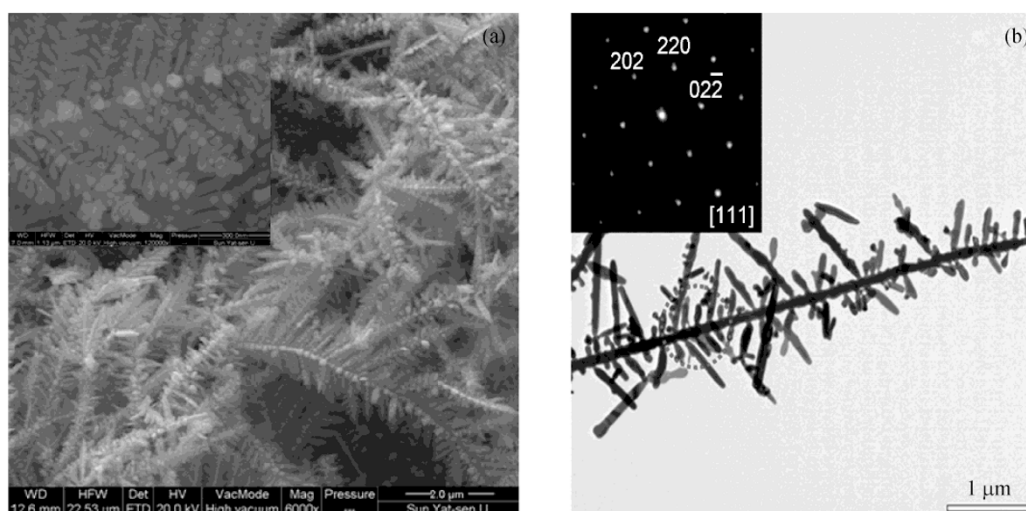


FIG. 7. Morphology of the as-deposits obtained by potentiostatic electrolysis on the Ti plates in AgNO_3 ($5 \times 10^{-3} \text{ mol L}^{-1}$)-SDS (0.2 g L^{-1}) aqueous solution at -3.00 V for 30 min. (a) SEM image of the dendrites, showing the attachment of nanoparticles, (b) TEM image of a single dendrite and the corresponding SAED pattern (the inset) taken along $[111]$ zone axis of fcc silver.

dendrite has two-dimensional structure with trunk and branches. The side branches are well symmetric and make an angle of about 60° with the trunk. It is found that the diameter of the trunk and the side branches is about 200 nm and 100 nm, respectively. A single dendrite structure shown in the inset of Fig. 7a indicates that some nanoparticles with the diameter of about 35 nm are attached on the surface of the trunk and branches. Figure 7b shows the TEM image of an individual silver dendrite with pine-like shape. The corresponding SAED pattern (the inset) obtained from the circle region in Fig. 7b shows six sharp spots, corresponding to the $\{220\}$ diffractions of single crystal fcc silver. The SAED results suggest that the branched structure is single crystalline with cubic phase and the side branches grow along $\{220\}$ directions.

The former reports [8-10,18,26,33] have demonstrated that the concentration of AgNO_3 plays a significant role in the formation of Ag dendrite. However, in the current investigation, although the solution condition was kept the same, different morphologies were obtained via changing the substrate. In this regard, it can be assumed that the mismatch degree of crystal lattice parameters between the substrate and the deposits may lead to different morphologies. The growth mode and the structures of the materials, to a great extent, depend on the interaction between the atoms of the substrates and that of the deposits. According to the diffusion limited aggregation (DLA) model, dendrites are formed by the aggregation of small particles [22]. In the early stage, Ag clusters are formed by initial attached aggregates which can align epitaxially with the substrate [37]. Compared with copper, the lattice parameter of titanium (pdf no.882321) is well match with that of silver (pdf no.870720). Therefore, in the stage of aggregation attachment, it seems to be more favorable for the occurrence of adhesion and aggregation of Ag clusters on Ti substrate than on Cu substrate. Once the aggregates contact on Ti substrate, they align epitaxially and serve as an immobile "seed" [38]. Then the generated particles stuck to a selected seed to form the dendrite structure as described by DLA model. Although the exact formation mechanism for the Ag dendrites is not quite clear at present, substrate plays an important role in the formation of well-defined Ag dendrite nanocrystals.

In summary, single crystalline silver nanoparticles with narrow size distribution and dendritic silver nanostructure have been prepared by potentiostatic electrodeposition in the assisted of ionized surfactant. It reveals that the morphologies of the structures are greatly influenced by the surfactant and substrate. In AgNO_3 -SDS aqueous solution, spherical nanoparticles with diameter of 30~35 nm were obtained on copper substrate, while silver dendrite nanostructures were obtained on titanium substrate. In the SDS-free solution, Ag nanoparticles were aggregated to form tower-like structure. It is found that the morphologies of silver nanostructures prepared by electrodeposition can be easily controlled via changing the substrate.

This work was supported by the National Foundations of China-Australia Special Fund for Scientific and Technological Cooperation (grant No. 20711120186), the Natural Science Foundations of China (grant No. 20873184), the Natural Science Foundations of Guangdong Province (grant No. 8151027501000095), the Science and Technology plan Projects of Guangdong Province (grant No. 2008B010600040) and the Instrumental Technique Research Foundation of Instrumental Analysis and Research Center, Sun Yat-sen University (grant No. 2009006).

Received 7 January 2010; accepted 5 February 2010; published online 28 February 2010.

References

1. L. Hueso and N. Mathur, *Nature* 427, 301 (2004). doi:10.1038/427301a
2. Y. Sun and Y. Xia, *Science* 298, 2176 (2002). doi:10.1126/science.1077229
3. N. Pinna, K. Weiss, J. Urban and M. P. Pileni, *Adv. Mater.* 13, 261 (2001). doi:10.1002/1521-4095(200102)13:4<261::AID-ADMA261>3.0.CO;2-X

4. J. S. Bradley, B. Tesche, W. Busser, M. Masse and M. T. Reetz, *J. Am. Chem. Soc.* 122, 4631 (2000). [doi:10.1021/ja992409y](https://doi.org/10.1021/ja992409y)
5. J. J. Mock, M. Barbic, D. R. Smith, D. A. Schultz and S. Schultz, *J. Chem. Phys.* 116, 6755 (2002). [doi:10.1063/1.1462610](https://doi.org/10.1063/1.1462610)
6. M. V. Roldan, A. Frattini, O. D. Sanctis, H. Troiani and N. Pellegrini, *Appl. Surf. Sci.* 254, 281 (2007). [doi:10.1016/j.apsusc.2007.07.059](https://doi.org/10.1016/j.apsusc.2007.07.059)
7. L. A. Gómez, C. B. De-Araújo, S. A. M. Brito and A. Galembek, *J. Opt. Soc. Of. Am. B: Opt. Phys.* 24, 2136 (2007). [doi:10.1364/JOSAB.24.002136](https://doi.org/10.1364/JOSAB.24.002136)
8. Y. Zhou, S. H. Yu, C. U. Wang, X. G. Li, U. R. Zhu and Z. Y. Chen, *Adv. Mater.* 11, 850 (1999). [doi:10.1002/\(SICI\)1521-4095\(199907\)11:10<850::AID-ADMA850>3.0.CO;2-Z](https://doi.org/10.1002/(SICI)1521-4095(199907)11:10<850::AID-ADMA850>3.0.CO;2-Z)
9. X. L. Gao, G. H. Gu, Z. S. Hu, Y. Guo, X. Fu and J. M. Song, *Colloids. Surf. A* 254, 57 (2005). [doi:10.1016/j.colsurfa.2004.11.009](https://doi.org/10.1016/j.colsurfa.2004.11.009)
10. J. Fang, H. You, P. Kong, Y. Yi, X. P. Song and B. J. Ding, *Cryst. Growth. Des.* 7, 864 (2007). [doi:10.1021/cg0604879](https://doi.org/10.1021/cg0604879)
11. Y. Y. Sun, D. Wang, J. G. Gao, Z. Zheng and Q. J. Zhang, *J. Appl. Polym. Sci.* 103, 3701 (2007). [doi:10.1002/app.24907](https://doi.org/10.1002/app.24907)
12. S. Chen, Z. Fan and D. L. Carroll, *J. Phys. Chem. B* 108, 5500 (2004). [doi:10.1021/jp031077n](https://doi.org/10.1021/jp031077n)
13. V. Alt, T. Bechert, P. Steinrücke, M. Wagener, P. Seidel, E. Dingeldein, E. Domann and R. Schnettler, *Biomaterials* 25, 4383 (2004). [doi:10.1016/j.biomaterials.2003.10.078](https://doi.org/10.1016/j.biomaterials.2003.10.078)
14. E. Vernè, S.D. Nunzio, M. Bosetti, P. Appendino, C.V. Brovarone, G. Maina and M. Cannas, *Biomaterials* 26, 5111 (2005). [doi:10.1016/j.biomaterials.2005.01.038](https://doi.org/10.1016/j.biomaterials.2005.01.038)
15. J. Yin, Y. Zhang, G. F. Yin and P. Zhang, *Key. Eng. Mater.* 336, 2115 (2007). [doi:10.4028/www.scientific.net/KEM.336-338.2115](https://doi.org/10.4028/www.scientific.net/KEM.336-338.2115)
16. J. J. Blaker, S. N. Nazhat and A. R. Boccaccini, *Biomaterials* 25, 1319 (2004). [doi:10.1016/j.biomaterials.2003.08.007](https://doi.org/10.1016/j.biomaterials.2003.08.007)
17. S. Wei, Y. Cheng, H. Jia, W. Xu and B. Zhao, *J. Colloid. Interface. Sci.* 298, 765 (2006). [doi:10.1016/j.jcis.2006.01.037](https://doi.org/10.1016/j.jcis.2006.01.037)
18. X. Q. Wang, K. Naka, H. Itoh, S. Park and Y. Chujo, *Chem. Comm.* 12, 1300 (2002). [doi:10.1039/b203185j](https://doi.org/10.1039/b203185j)
19. L. T. Qu and L. M. Dai, *J. Phys. Chem. B* 29, 13985 (2005). [doi:10.1021/jp0515838](https://doi.org/10.1021/jp0515838)
20. V. S. Kumar, B. M. Nagaraja, V. Shashikala, A. H. Padmasri, S. S. Madhavendra, B. Raju and K. S. Rama, *J. Mol. Cat. A: Chem.* 223, 313 (2004). [doi:10.1016/j.molcata.2003.09.047](https://doi.org/10.1016/j.molcata.2003.09.047)
21. P. M. Shirage, D. D. Shivagan, L. A. Ekal, N. V. Desai, S. B. Mane and S. H. Pawar, *Appl. Surf. Sci.* 182, 403 (2001). [doi:10.1016/S0169-4332\(01\)00459-7](https://doi.org/10.1016/S0169-4332(01)00459-7)
22. S. Wang and H. Xin, *J. Phys. Chem. B* 104, 5681(2000). [doi:10.1021/jp000225w](https://doi.org/10.1021/jp000225w)
23. Q. Yang, F. Wang, K. Tang, C. Wang, Z. Chen and Y. Qian, *Mater. Chem. Phys.* 78, 495 (2003). [doi:10.1016/S0254-0584\(02\)00379-6](https://doi.org/10.1016/S0254-0584(02)00379-6)
24. J. P. Xiao, Y. Xie, R. Tang, M. Chen and X. B. Tian, *Adv. Mater.* 13, 1887 (2001). [doi:10.1002/1521-4095\(200112\)13:24<1887::AID-ADMA1887>3.0.CO;2-2](https://doi.org/10.1002/1521-4095(200112)13:24<1887::AID-ADMA1887>3.0.CO;2-2)
25. H. F. Gong and M. H. Liu, *Chem. Mater.* 14, 4933 (2002). [doi:10.1021/cm020232s](https://doi.org/10.1021/cm020232s)
26. Y. C. Zhu, H. G. Zheng, Y. Li, L. S. Gao, Z. P. Yang and Y. T. Qian, *Mater. Res. Bull.* 38, 1829 (2003). [doi:10.1016/j.materresbull.2003.08.004](https://doi.org/10.1016/j.materresbull.2003.08.004)
27. G. Cardini and M. Muniz-Miranda, *J. Phys. Chem. B* 106, 6875 (2002). [doi:10.1021/jp0142051](https://doi.org/10.1021/jp0142051)
28. M. Oliveira and I. A. Carlos, *J. Appl. Electrochem.* 39, 1217 (2009). [doi:10.1007/s10800-009-9777-6](https://doi.org/10.1007/s10800-009-9777-6)
29. N. Yanagihara, Y. Tanaka and H. Okamoto, *Chem. Lett.* 8, 796 (2001). [doi:10.1246/cl.2001.796](https://doi.org/10.1246/cl.2001.796)
30. H. S. Wang, X. L. Qiao, J. G. Chen, X. J. Wanga and S. Y. Ding, *Mater. Chem. Phys.* 94, 449 (2005). [doi:10.1016/j.matchemphys.2005.05.005](https://doi.org/10.1016/j.matchemphys.2005.05.005)
31. J. J. Zhu, S. W. Liu, O. Palchik, Y. Kolytyn and A. Gedanken, *Langmuir* 16, 6396 (2000). [doi:10.1021/la991507u](https://doi.org/10.1021/la991507u)
32. Z. H. Kang, E. B. Wang, S. Y. Lian, B. D. Mao, C. Lei and X. Lin, *Mater. Lett.* 59, 2289 (2005). [doi:10.1016/j.matlet.2005.03.005](https://doi.org/10.1016/j.matlet.2005.03.005)
33. J. J. Zhu, X. H. Liao and H. Y. Chen, *Mater. Res. Bull.* 36, 1687 (2001). [doi:10.1016/S0025-5408\(01\)00600-6](https://doi.org/10.1016/S0025-5408(01)00600-6)
34. T. S. Ahmadi, Z. L. Wang, T. C. Green, A. Henglein and M. A. El-Sayed, *Science* 272, 1924 (1996). [doi:10.1126/science.272.5270.1924](https://doi.org/10.1126/science.272.5270.1924)
35. Z. A. Peng and X. G. Peng, *J. Am. Chem. Soc.* 123, 1389 (2001). [doi:10.1021/ja0027766](https://doi.org/10.1021/ja0027766)
36. H. H. Huang, X. P. Ni, G. L. Loy, C. H. Chew, K. L. Tan, F. C. Loh, J. F. Deng and G. Q. Xu, *Langmuir* 12, 909 (1996). [doi:10.1021/la950435d](https://doi.org/10.1021/la950435d)
37. J. F. Banfield, S. A. Welch, H. Z. Zhang, T. T. Ebert and R. L. Penn, *Science* 289, 751 (2000). [doi:10.1126/science.289.5480.751](https://doi.org/10.1126/science.289.5480.751)
38. X. P. Sun and M. Hagner, *Langmuir* 23, 9147 (2007). [doi:10.1021/la701519x](https://doi.org/10.1021/la701519x)